

PAPER

Super persistent transient in a master–slave configuration with Colpitts oscillators

To cite this article: R C Bonetti *et al* 2014 *J. Phys. A: Math. Theor.* **47** 405101

View the [article online](#) for updates and enhancements.

You may also like

- [Design and measurement of a 53 GHz balanced Colpitts oscillator](#)
Zhao Yan, Wang Zhigong, Li Wei *et al.*
- [Modeling of interface roughness in thermoelectric composite materials](#)
F Gather, C Heiliger and P J Klar
- [Thermal Characteristics at Interface of Bi₂Te₃/Sb₂Te₃ Superlattices](#)
Fumiaki Takahashi, Yukihiro Hamada, Takatoshi Mori *et al.*



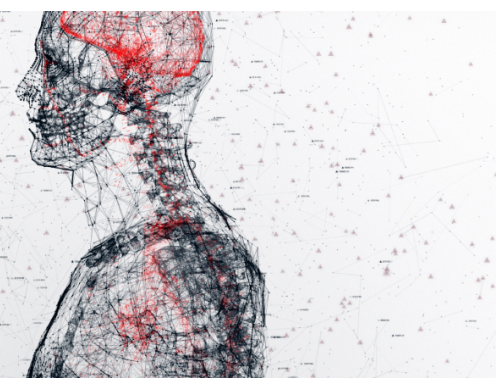
physicsworld

AI in medical physics week

20–24 June 2022

Join live presentations from leading experts
in the field of AI in medical physics.

physicsworld.com/medical-physics



Super persistent transient in a master–slave configuration with Colpitts oscillators

R C Bonetti¹, S L T de Souza², A M Batista³, J D Szezech Jr³,
I L Caldas⁴, R L Viana⁵, S R Lopes⁵ and M S Baptista⁶

¹ Pós-Graduação em Ciências, Universidade Estadual de Ponta Grossa, 84030-900, Ponta Grossa, Paraná, Brazil

² Departamento de Física e Matemática, Universidade Federal de São João del Rei, 36420-000, Ouro Branco, Minas Gerais, Brazil

³ Departamento de Matemática e Estatística, Universidade Estadual de Ponta Grossa, 84030-900, Ponta Grossa, Paraná, Brazil

⁴ Instituto de Física, Universidade de São Paulo, Caixa Postal 66316, 05315-970, São Paulo, SP, Brazil

⁵ Departamento de Física, Universidade Federal do Paraná, 81531-990, Curitiba, Paraná, Brazil

⁶ Institute for Complex Systems and Mathematical Biology, SUPA, University of Aberdeen, Aberdeen AB24 3UE, UK

E-mail: antoniomarcosbatista@gmail.com

Received 1 May 2014, revised 24 July 2014

Accepted for publication 19 August 2014

Published 23 September 2014

Abstract

Master–slave systems have been intensively investigated for modelling the application of chaos in communications. We considered Colpitts oscillators coupled according to a master–slave configuration in order to study chaos synchronization. We revealed the existence of superpersistent transients in this coupled system. The transient is a ubiquitous phenomenon in nonlinear dynamical systems, and it is responsible for important physical phenomena. We characterized superpersistent transients through a scaling law for their average lifetime. Unstable–unstable pair bifurcation has been identified as the generic mechanism for these transients. Moreover, we showed that an additive noise, added to the slave system, may suppress the chaos synchronization. Our results show that synchronization can be achieved for higher coupling strength when there is noise. However, the noise may induce a longer transient if the synchronization is not suppressed.

Keywords: Colpitts, synchronisation, master-slave

PACS numbers: 05.45.-a, 05.45.Xt

(Some figures may appear in colour only in the online journal)

1. Introduction

Coupled chaotic systems can synchronize their trajectories [1]. The synchronization of coupled chaotic systems has important applications in many fields, such as biological systems [2], secure communications [3], and chemical reactions [4]. The phenomenon of chaos synchronization may occur when two or more dissipative chaotic systems are coupled. It is often understood as a behaviour in which coupled chaotic systems exhibit not only identical but also chaotic oscillations. Synchronized chaotic systems have been considered in various studies, with interesting applications in signal processing and communication.

Recent works have shown that chaos synchronization for a master–slave configuration is relevant to communication systems. The slave system is driven by a signal derived from the master [5]. Master–slave synchronization schemes have been reported in experimental and theoretical studies which introduce the possibility of applying chaotic synchronization in communication. Communication security schemes may be based on chaos synchronization: message signals are injected into a transmitter, then encrypted, and transmitted to a receiver; the synchronization of the chaos is required to recover the message.

Here we focus our study on two chaotic coupled Colpitts oscillators [6]. The Colpitts oscillator was invented by engineer Edwin Henry Colpitts [7]. It is a damped resonant circuit with two capacitors, an inductor, and a bipolar junction transistor. This circuit provides an occasional driving force via a nonlinear switching action. We chose this circuit due to the fact that it can be useful in applications in communication systems, as well as exhibiting a rich dynamical behaviour for certain parameter values. De Feo and collaborators identified various families of limit cycles and bifurcations. They also demonstrated that the bifurcation diagram in the parameter space is organized through an infinite family of homoclinic bifurcations [8]. In the Colpitts oscillator the operation frequency can vary from a few hertz up to the microwave frequency range, a characteristic that enables the use of this circuit to transmit information in channels with difference frequency bandwidths.

There has been a great interest in the study of synchronization and control of Colpitts oscillators. Control schemes have been used to suppress chaos. Li and collaborators used a controller to drive a chaotic Colpitts system to a desired state [9]—that is, to achieve the stabilization of the chaotic motion to a steady state. In another work, the circuit was controlled by using a nonlinear feedback [10]. Synchronization between chaotic Colpitts systems has been found in identical and mismatched cases [11, 12]. Furthermore, there are works concerning the synchronization of Colpitts oscillators that operate in ultrahigh frequency ranges [13].

In this article, we study two coupled Colpitts oscillators in a master–slave configuration and focus our attention on chaos synchronization. Our main objective is to verify the existence of superpersistent chaotic transients [14, 15], and the effect of noise on the synchronous behaviour [16, 17]. Superpersistent transients are characterized by a scaling law for their average lifetime. Grebogi and collaborators [14] identified an unstable–unstable pair bifurcation as the dynamical mechanism for these transients. Superpersistent transients may accompany phenomena such as the onset of riddled basins, as well as the stability of attractors formed from inertial particles advected in hydrodynamical fluid flows [18, 19]. Noise can produce significant effects in chaotic systems. In fact, noise can induce superpersistent transients [20]. Noise-induced synchronization has been studied in the effects of small-world connectivity on noise-induced temporal and spatial order in neural media [21]. Moreover, persistency of noise-induced spatial periodicity in excitable media has been reported [22].

This article is organized as follows. In section 2 we present the coupled Colpitts oscillators. In section 3 we study the onset of synchronization and show the existence of

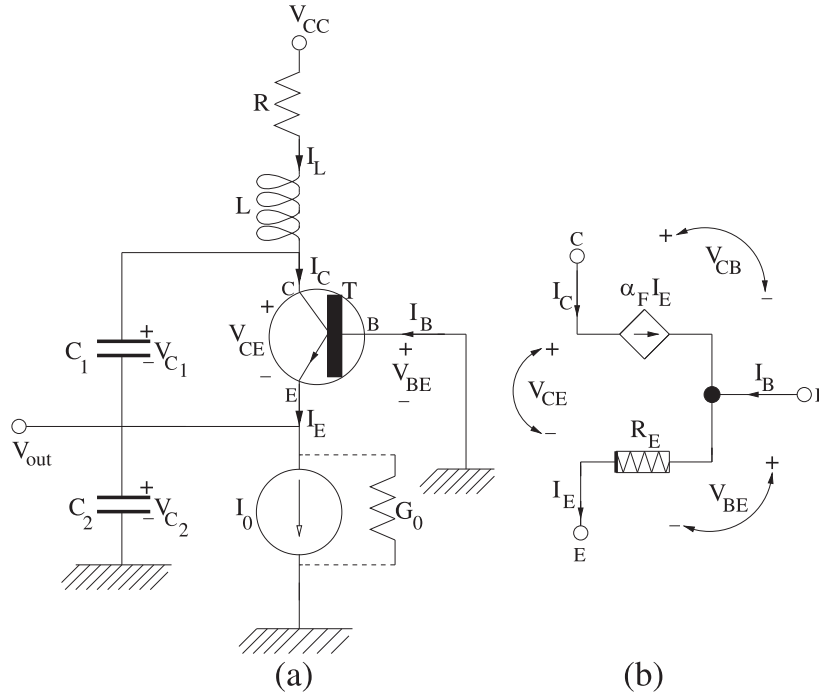


Figure 1. The circuit diagram of a Colpitts oscillator. (a) The circuit configuration and (b) the bipolar junction transistor (BJT).

superpersistent transients. In section 4 we describe the effect of noise on the system. The last section contains our conclusions.

2. The Colpitts oscillator

The Colpitts oscillator is a type of resonant circuit with a transistor for feedback. This oscillator has been used in electronic devices and communication systems, due to the fact that it can exhibit chaos [23]. Figure 1(a) exhibits the circuit configuration containing a bipolar junction transistor (BJT), according to figure 1(b). The state equations are given by

$$\begin{aligned}
 C_1 \frac{dV_{C_1}}{dt'} &= -\alpha_F f(-V_{C_2}) + I_L, \\
 C_2 \frac{dV_{C_2}}{dt'} &= (1 - \alpha_F) f(-V_{C_2}) - G_0 V_{C_2} + I_L - I_0, \\
 L \frac{dI_L}{dt'} &= -V_{C_1} - V_{C_2} - R I_L + V_{CC},
 \end{aligned} \tag{1}$$

where the voltages V_{C_1} and V_{C_2} are associated with the capacitors C_1 and C_2 , respectively, V_{CC} is the voltage supply, I_L is the current through the inductor L and t is the time. There is a current generator I_0 to maintain a constant biasing emitter current. The function $f()$ is the driving point characteristic of the nonlinear resistor R_E and it can be expressed as $I_E = f(V_{C_2}) = f(-V_{BE})$, where α_F is the common-base forward short-circuit gain.

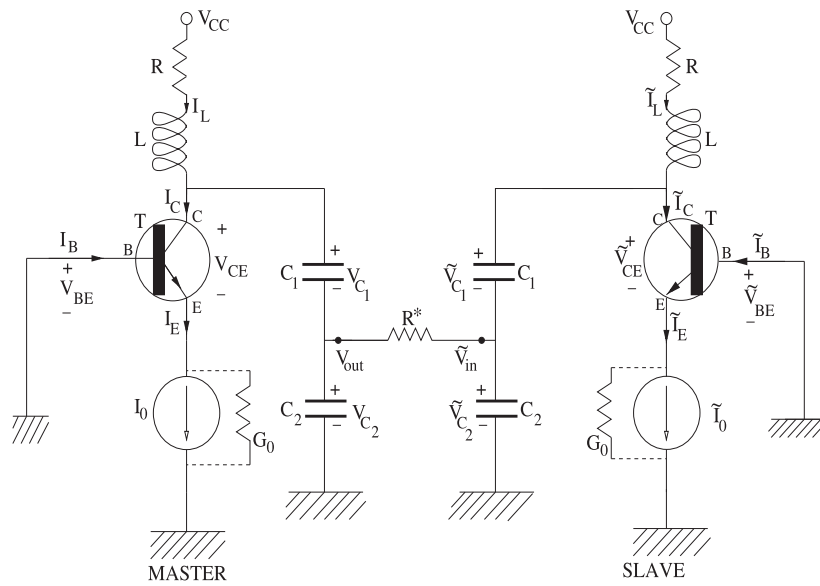


Figure 2. The circuit diagram of a coupled Colpitts system with a master–slave configuration.

We consider two Colpitts oscillators in a master–slave configuration, in accordance with the scheme shown by figure 2. If this coupled system were to be used for communication purposes, the transmitter would be the master and the receiver the slave. We also consider noise in the channel.

Introducing the following dimensionless variables

$$\begin{aligned}
 x_1 &= \frac{V_{C_1} - \bar{V}_{C_1}}{V_T}, \\
 x_2 &= \frac{V_{C_2} - \bar{V}_{C_2}}{V_T}, \\
 x_3 &= \frac{I_L - \bar{I}_L}{I_0},
 \end{aligned} \tag{2}$$

where

$$\bar{V}_{C_1} = V_{CC} - \alpha_F R f(-\bar{V}_{C_2}) - \bar{V}_{C_2}, \tag{3}$$

$$\bar{V}_{C_2} = \frac{1}{G_0} [n(-\bar{V}_{C_2}) - I_0] \tag{4}$$

$$\bar{I}_L = -\alpha_F f(-\bar{V}_{C_2}), \tag{5}$$

we obtain the equations for a unidirectional master–slave configuration

$$\begin{aligned}\frac{dx_1}{dt} &= \frac{g}{Q(1-k)} [-\alpha_F n(x_2) + x_3], \\ \frac{dx_2}{dt} &= \frac{g}{Qk} [(1-\alpha_F)n(x_2) + x_3], \\ \frac{dx_3}{dt} &= -\frac{Qk(1-k)}{g} [x_1 + x_2] - \frac{1}{Q}x_3, \\ \frac{dy_1}{dt} &= \frac{g}{Q(1-k)} [-\alpha_F n(y_2) + y_3], \\ \frac{dy_2}{dt} &= \frac{g}{Qk} [(1-\alpha_F)n(y_2) + y_3] + \varepsilon [x_2 - y_2],\end{aligned}\tag{6}$$

$$\begin{aligned}\frac{dy_3}{dt} &= -\frac{Qk(1-k)}{g} [y_1 + y_2] - \frac{1}{Q}y_3, \\ t &= t'\omega_0,\end{aligned}\tag{7}$$

$$\omega_0 = \frac{1}{\sqrt{L\frac{C_1C_2}{C_1+C_2}}},\tag{8}$$

where x_1 , x_2 and x_3 belong to the master circuit, y_1 , y_2 and y_3 belong to the slave circuit, and ω_0 is the resonant frequency of the tank circuit due to L , C_1 and C_2 . The time derivative of y_2 containing the coupling term depends on variables of both circuits. The nonlinear terms are given by $n(x) = e^{-x} - 1$ and $n(y) = e^{-y} - 1$. The dimensionless parameters are

$$Q = \frac{\omega_0 L}{R},\tag{9}$$

$$k = \frac{C_2}{C_1 + C_2},\tag{10}$$

$$g = \frac{I_0 L}{V_T R (C_1 + C_2)},\tag{11}$$

and ε is the coupling strength, which is defined as $\varepsilon = \sqrt{L/C_1} R^{*-1}$. We use $k = 0.5$, $\alpha_F = 0.996$, $R = 80 \Omega$, $C_1 = C_2 = 1 \mu\text{F}$, $L = 18.2 \mu\text{H}$, $V_T = 27 \text{ mV}$, and $Q = 1.77$. With these values set and $g = 2.863$, the Colpitts oscillator presents chaotic behaviour. The system presents a broad range of different dynamical regimes as the parameter g is varied, such as chaotic behaviour, periodic solutions, Hopf bifurcation, and coexistence of solutions. In this work, in order to study chaos synchronization, we consider a small interval of the values of g such that the system only presents chaotic behaviour.

3. Chaos synchronization

Chaotic systems have applications in secure and spread spectrum communications. Previous works have presented applications of chaos synchronization in wireless communications [24] and multiplexing mixed chaotic signals generated by different electronic oscillators [25]. Chaos synchronization occurs when the state variables of the two circuits are equal. Such a

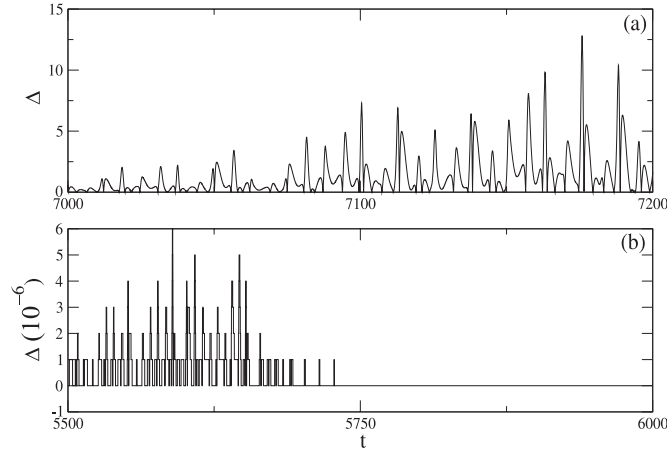


Figure 3. Time evolution of the synchronization error considering (a) $\epsilon = 0.05$ and (b) $\epsilon = 0.089$.

condition is achieved after a transient time that depends on the stability of the synchronization manifold.

A numerical diagnostic allowing statements to be made about the synchronous state is provided by the synchronization error

$$\Delta = |x_1 - y_1|. \tag{12}$$

Figure 3 shows the time evolution of Δ for two situations: (a) when there is no synchronization between the Colpitts oscillators and (b) when there is chaos synchronization. When the oscillators are completely synchronized we have $\Delta = 0$. If the system presents chaos synchronization, the synchronization errors $\Delta = |x_2 - y_2|$ and $\Delta = |x_3 - y_3|$ will exhibit the same result.

We investigate the dependence of the synchronization error on the control parameter g and the coupling strength ϵ . Using the time-averaged error

$$\bar{\Delta} = \frac{1}{t_2 - t_1} \sum_{t_1}^{t_2} \Delta(t), \tag{13}$$

where $t_2 - t_1$ is the time window for measurements, chaos synchronization is stated to occur when $\bar{\Delta} < 10^{-4}$. We consider $t_1 = 5000$ and $t_2 = 10\,000$, but similar results were obtained for $t_1 = 18\,000$ and $t_2 = 20\,000$. Figure 4 shows a parameter space, indicating by the colours regions of parameters that lead to no synchronization (white) and regions of parameters that lead to synchronization (green), representing parameters for which $\bar{\Delta} < 10^{-4}$.

We calculate the spectrum of Lyapunov exponents of the synchronization manifold and its transverse directions in order to verify the local stability of the synchronization manifold. We obtain the spectrum considering the same initial conditions for the two circuits: $x_1 = y_1 = 0.02$, $x_2 = y_2 = 10^{-4}$ and $x_3 = y_3 = 10^{-4}$. We are interested in the largest two Lyapunov exponents. When the maximal exponent is positive and the second largest is negative, the system presents chaos synchronization [26]. The synchronization manifold is locally stable, since the negative exponent measures how perturbation propagates along the direction transverse to the synchronization manifold. Consequently, the circuits can

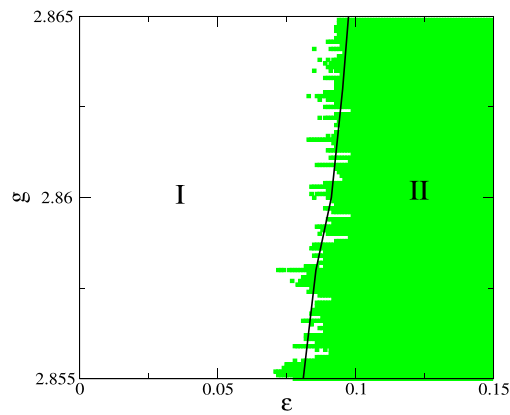


Figure 4. Synchronized domains (green region) in the g - ϵ parameter plane. The black line separates the regions for which the synchronization manifold is unstable (I) and stable (II). Stability is measured via the Lyapunov exponents of the synchronization manifold.

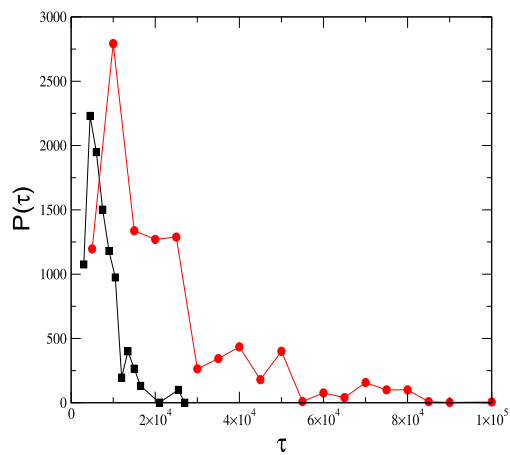


Figure 5. Histogram of the transient time intervals for a total of 10^4 different initial conditions for x_2 and y_2 in the interval $[0, 0.001]$, where we consider $g = 2.863$, $\epsilon = 0.086$ (red circles) and $\epsilon = 0.090$ (black squares).

synchronize. The black line, shown in figure 4, separates two regions. In region I the coupled oscillators do not synchronize, while in region II synchronization occurs.

We can see in figure 4 that the boundary between the two regions has an irregular pattern. This suggests the existence of an entangled basin boundary for the synchronous attractor [27]. Consequently, the time taken to reach the synchronous state will strongly depend on the initial conditions, some of them being responsible for very long transients. The transient time is denoted by τ , and its average value is τ_M .

The histogram of the transient time for an ensemble of initial conditions is shown in figure 5, where the red circles correspond to $\epsilon = 0.090$ and the black squares to $\epsilon = 0.086$. The statistical distribution of the transient sizes was obtained by considering 10^4 different initial conditions for x_2 and y_2 , and shows that small transients become more common when

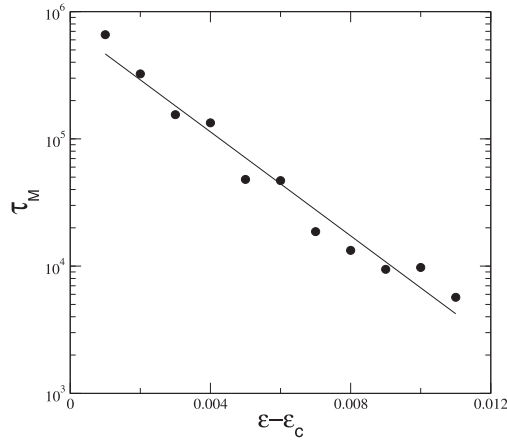


Figure 6. Scaling of the superpersistent transient on varying the coupling strength, for $g = 2.863$ and $\epsilon_c = 0.078$. Each point represents the average over 100 different initial conditions for x_2 and y_2 . The solid line is an exponential fitting with exponent -470.31 . The value of ϵ_c is obtained when the synchronization manifold becomes stable.

the value of the coupling strength increases. Therefore, for some values of g and ϵ , around the region of the boundary in the green area of figure 4, the circuits may present large transients, depending on the initial conditions.

Here we recall that there is a distinct class of chaotic transients that are referred to as superpersistent [14, 15]. Such transient times are characterized by the following scaling law for their average transient

$$\tau_M \sim \exp \left[\beta (p - p_c)^{-\gamma} \right], \tag{14}$$

where β and γ are positive constants, p_c is a critical parameter value, and the transient occurs for $p > p_c$. In this work the critical parameter is the coupling strength. The least-squares fit in figure 6 exhibits an exponential distribution for τ_M and $\epsilon - \epsilon_c$, which indicates a superpersistent transient with exponent $\gamma = 1$.

The mechanism for a persistent transient is an unstable–unstable pair bifurcation [28]. After this bifurcation the trajectory spends a time $T(p)$ in the channel centred about an earlier existing unstable periodic orbit. The basic dynamics can be described by

$$\frac{dx}{dt} = x^{\psi-1} + p. \tag{15}$$

The tunnelling time is given by

$$T(p) \approx \int_0^l \frac{dx}{x^{\psi-1} + p} \sim p^{\frac{\psi-2}{\psi-1}}, \tag{16}$$

where the root of the channel is $x = 0$, and l is its length. Then, substituting equation (16) into the average transient lifetime, which is associated with the tunnelling time via $\tau_M(p) \sim \exp(\beta T(p))$, we obtain

$$\tau_M \sim \exp \left(\beta p^{-\frac{\psi-2}{\psi-1}} \right), \tag{17}$$

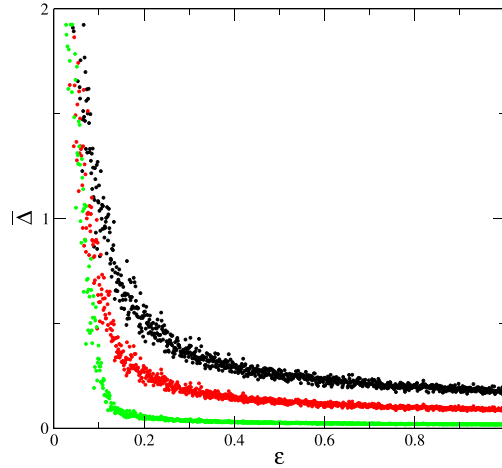


Figure 7. Synchronization error versus coupling strength for $g = 2.863$, $A = 0.1$ (green circles), $A = 0.5$ (red circles) and $A = 1.0$ (black circles). These three cases have exactly the same initial conditions.

where $\beta > 0$ is a constant, and $(\psi - 2)/(\psi - 1) < 1$. Therefore, the average transient lifetime diverges in an exponential algebraic way [29].

4. The effect of noise

We analyse chaos synchronization under realistic conditions, with noise in the experiments [30]. We add a stochastic perturbation to the variable $y_2(t)$ of equation (6)

$$\frac{dy_2}{dt} = \frac{g}{Qk} \left[(1 - \alpha_F)n(y_2) + y_3 \right] + \varepsilon[x_2 - y_2] + Ar(t), \quad (18)$$

where A is the level of the stochastic perturbation and $r(t)$ is a pseudorandom variable. We consider a random number generator that returns a normally distributed deviate with zero mean and unit variance. In other words, the noise is a white Gaussian noise (AWGN) [31].

To understand the effect of noise under the synchronization conditions, we measure the synchronization error for different values of the noise level and the coupling strength. In figure 7, we plot the time-averaged synchronization error versus the coupling strength for three values of the noise level. When the noise level is small (green circles) the value of the time-averaged error decreases sharply when the coupling strength increases. For larger values of A (red and black circles) the time-averaged error decays less abruptly as a function of ε . For all situations, $\bar{\Delta} > 0$, showing that synchronization is suppressed.

Synchronization is affected by noise. In figure 8 we consider the same parameters as were adopted in figure 4 but add noise with level $A = 3 \times 10^{-5}$. Comparing figure 8 (with noise) with figure 4 (without noise), it is possible to observe that due to the effect of the noise, a larger value of ε is necessary to make the systems synchronize. Like for figure 4, the structure of the boundary between the synchronous region and the nonsynchronous region is a consequence of the existence of an entangled basin boundary that produces superpersistent transients. We obtain the synchronized region by checking whether $\bar{\Delta} < 10^{-4}$, for $t_1 = 1000$ and $t_2 = 20\,000$. We analyse the noise effect on the synchronized region, fixing the value of g

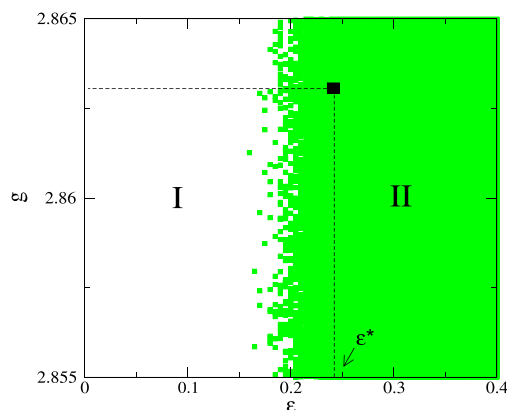


Figure 8. Synchronized domains (green region), considering the same parameters as for figure 4, and a small noise $A = 3 \times 10^{-5}$.

and varying the noise amplitude A , to obtain the ε^* for which the average transient τ_M is approximately 10^4 (figure 9(a)). Therefore, the larger the noise amplitude is, the larger the coupling strength must be to synchronize.

The phenomenon of the superpersistent transient is affected by the noise; that is, a small noise leads to an increased transient time. Figure 9(b) shows histograms for $g = 2.863$, $\varepsilon = 1$, $A = 5 \times 10^{-5}$ (black circles) and $A = 6 \times 10^{-5}$ (red squares), in order to show that the noise induces longer transients. When $A \leq 4 \times 10^{-5}$ the transients have values around 10^3 . Moreover, for $A \geq 7 \times 10^{-5}$ the noise may suppress chaos synchronization. It is worthy of comment that near the critical parameter ε_c , the average transient τ_M quickly increases when the noise amplitude grows, according to an exponential relationship $\tau_M \sim \phi \exp(\varphi A)$, where ϕ and φ are positive constants.

5. Conclusions

In this paper, we have studied some aspects of the chaos synchronization displayed by two coupled Colpitts systems with a master–slave configuration. We obtained a set of parameters which may lead the coupled circuits to adopt a synchronized or a nonsynchronized state. We verified the existence of superpersistent transients. Such transients are mainly situated in the border of the synchronized domain in the parameter space of g versus ε , where g is the loop gain of the oscillator, and ε is the coupling strength.

The effects of noise on the coupled circuits were considered. Noise acts on the system in such a way that synchronization can only be achieved for higher coupling strength. Moreover, the transients become longer.

Our results enable us to predict a set of parameters for the coupled Colpitts oscillators needed to observe superpersistent transients that can be used in laboratory experiments. The persistent transients described are similar to those observed in dissipative systems, and should be related to the chaotic saddle of the coupled systems [32, 33]. Moreover, the analysis realized in this work can be extended to application to other oscillators. Superpersistent chaotic transients have been observed in coupled Chua circuits and coupled Rössler oscillators [15].

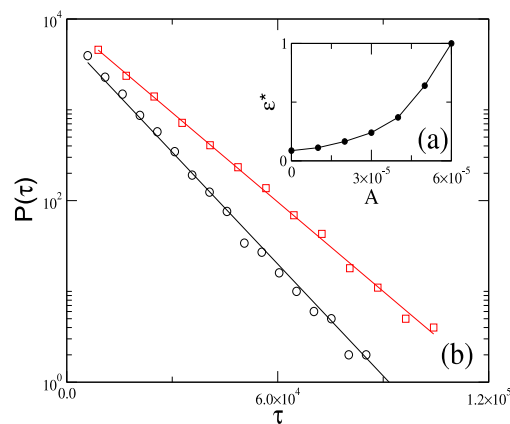


Figure 9. (a) ε^* versus A , where the black circles correspond to $\tau_M \approx 10^4$. (b) Histograms for the transient time considering $g = 2.863$, $\varepsilon = 1$, $A = 5 \times 10^{-5}$ (black circles) and $A = 6 \times 10^{-5}$ (red squares).

In future works, we plan to study such coupled systems considering electronic simulations [34], and also to obtain experimental results through the use of an electronic circuit.

Acknowledgments

This work was made possible by financial support from the following Brazilian government agencies: CNPq, CAPES, Fundação Araucária (Paraná) and FAPESP. M S Baptista acknowledges EPSRC-EP/I032606/1.

References

- [1] Pecora L M and Carrol T L 1990 Synchronization in chaotic systems *Phys. Rev. Lett.* **64** 821–4
- [2] Batista C A S, Lameu E L, Batista A M, Lopes S R, Pereira T, Zamora-López G, Kurths J and Viana R L 2012 Phase synchronization of bursting neurons in clustered small-world networks *Phys. Rev. E* **8** 016211
- [3] Yang J Q and Zhu F L 2013 Synchronization for chaotic systems and chaos-based secure communications via both reduced-order and step-by-step sliding mode observers *Commun. Nonlinear Sci. Numer. Simulat.* **18** 926–37
- [4] Wang J-W and Chen A-M 2010 Partial synchronization in coupled chemical chaotic oscillators, *J. Comp. Appl. Math.* **233** 1897–904
- [5] Suykens J A K, Curran P F and Chu L O 1999 Robust synthesis for master-slave synchronization of Lur'e system *IEEE Trans. Circuits Syst. I Fundam. Theory Appl.* **46** 841
- [6] de Feo O, Maggio G M and Kennedy M P 2000 The Colpitts oscillator: families of periodic solutions and their bifurcations *Int. J. Bifurc. Chaos* **10** 935–58
- [7] Colpitts E H 1927 Oscillation generator *US Patent 1624537* 1–4
- [8] De Feo O and Maggio G M 2003 Bifurcations in the Colpitts oscillator: from theory to practice *Int. J. Bifurc. Chaos* **13** 2917–34
- [9] Li H G, Zhou S P and Yang K 2007 Controlling chaos in Colpitts oscillator *Chaos Solitons Fractals* **33** 582–7
- [10] Effa J Y, Essimbi B Z and Ngundam J M 2009 Synchronization of improved chaotic Colpitts oscillators using nonlinear feedback control *Nonlinear Dyn.* **58** 39–47
- [11] Baziliauskas A, Krivickas R and Tamasevicius A 2006 Coupled chaotic Colpitts oscillators: identical and mismatched cases *Nonlinear Dyn.* **44** 151–8

- [12] Mata-Machuca J L and Martínez-Guerra F 2012 Asymptotic synchronization of the Colpitts oscillator *Comp. Math. Appl.* **63** 1072–8
- [13] Kengne J, Chdjou J C, Kenne G and Kyamakya K 2012 Dynamical properties and chaos synchronization of improved Colpitts oscillators *Commun. Nonlinear Sci. Numer. Sim.* **17** 2914–23
- [14] Grebogi C, Ott E and Yorke J A 1985 Super persistent chaotic transients *Ergod. Th. Dynam. Sys.* **5** 341–72
- [15] Andrade V and Lai Y-C 2001 Super persistent chaotic transients in physical systems: effect of noise on phase synchronization of coupled chaotic oscillators *Int. J. Bifurc. Chaos* **11** 2607–19
- [16] De Souza S L T, Caldas I L, Viana R L, Batista A M and Kapitaniak T 2005 Noise-induced basin hopping in a gearbox model *Chaos Solitons Fractals* **26** 1523–31
- [17] De Souza S L T, Batista A M, Caldas I L, Viana R L and Kapitaniak T 2007 Noise-induced basin hopping in a vibro-impact system *Chaos Solitons Fractals* **32** 758–67
- [18] Do Y and Lai Y C 2003 Superpersistent chaotic transients in physical space: advective dynamics of inertial particles in open chaotic flows under noise *Phys. Rev. Lett.* **91** 224101
- [19] Do Y and Lai Y C 2004 Extraordinarily superpersistent chaotic transients *Europhys. Lett.* **67** 914–20
- [20] Do Y and Lai Y C 2005 Scaling laws for noise-induced superpersistent chaotic transients *Phys. Rev. E* **71** 046208
- [21] Perc M 2007 Effects of small-world connectivity on noise-induced temporal and spatial order in neural media *Chaos Solitons Fractals* **31** 280–91
- [22] Perc M 2005 Persistency of noise-induced spatial periodicity in excitable media *Europhys. Lett.* **72** 712–8
- [23] Kennedy M P 1994 Chaos in the Colpitts oscillator *IEEE Trans. Circuit Syst.* **41** 771–4
- [24] Sano E 2006 A chaotic wireless communication system based on collective synchronization among wireless nodes *IEICE Electronics Express* **3** 262–8
- [25] Zhi-Guo S, Li-Xin R and Kang-Sheng C 2005 Multiplexing chaotic signals generated by Colpitts oscillator and Chua circuit using dual synchronization *Chin. Phys. Lett.* **22** 1336–9
- [26] Gade P M, Cerdeira H A and Ramaswamy R 1995 Coupled maps on trees *Phys. Rev. E* **52** 2478–85
- [27] Camargo S, Viana R L and Anteneodo C 2012 Intermingled basins in coupled Lorenz systems *Phys. Rev. E* **85** 036207
- [28] Viana R L and Grebogi C 2000 Unstable dimension variability and synchronization of chaotic systems *Phys. Rev. E* **62** 462–8
- [29] Tél T and Lai Y C 2008 Chaotic transients in spatially extended systems *Phys. Rep.* **460** 245–75
- [30] Hong S, Shi Z, Wang L, Gu Y and Chen K 2012 Adaptive regularized particle filter for synchronization of chaotic Colpitts circuits in an SWGN channel *Circuits Syst. Signal Process.* 1–17
- [31] Shi Z, Hong S and Chen K 2008 Experimental study on tracking the state of analog Chua’s circuit with particle filter for chaos synchronization *Phys. Lett. A* **372** 5575–80
- [32] Kraut S and Feudel U 2002 Multistability, noise, and attractor hopping: the crucial role of chaotic saddles *Phys. Rev. E* **66** 015207(R)
- [33] Kraut S and Feudel U 2003 Noise-induced escape through a chaotic saddle: lowering of the activation energy *Physica D* **181** 222–34
- [34] Kenfack G and Tiedeu A 2013 Secured transmission of ECG signals: numerical and electronic simulations *J. Signal Inf. Process.* **4** 158–69